Research Paper

Machine learning developed a PI3K/Akt pathway-related signature for predicting prognosis and drug sensitivity in ovarian cancer

Xiaofang Han[1], Liu Yang[1], Hui Tian[1], Yuanyuan Ji[1]

[1]Core Laboratory, Shanxi Provincial People's Hospital (Fifth Hospital) of Shanxi Medical University, Taiyuan 030012, China

Correspondence to: Xiaofang Han; **email:** sldgng@163.com, https://orcid.org/0000-0001-7105-1292
Keywords: immunotherapy, prognostic signature, ovarian cancer, machine learning, PI3K/Akt pathway
Received: August 1, 2023 **Accepted:** September 18, 2023 **Published:** October 17, 2023

ABSTRACT

Background: Ovarian cancer is one of the deadliest malignancies among females, generally having a poor prognosis. The PI3K/Akt pathway plays a vital role in the oncogenesis and progression of many types of cancer. Limited studies have fully clarified the role of PI3K/Akt pathway in the prognosis of ovarian cancer and its correlation with drug sensitivity.

Methods: A prognostic PI3K/Akt pathway related signature (PRS) was constructed with 10 machine learning algorithms using TCGA, GSE14764, GSE26193, GSE26712, GSE63885 and GSE140082 datasets. Gaussian mixture and logistic regression were performed to identify the optimal models for classifying lymphatic and venous invasion.

Results: The optimal prognostic PRS developed by Lasso + survivalSVM algorithm acted as an independent risk factor for overall survival (OS) of ovarian cancer patients and had a good performance in evaluating OS rate of ovarian cancer patients. Significant correlation was obtained between PRS-based risk score and Immune score, ESTIMATE score, immune cells and cancer-related hallmarks. Low risk score indicated a lower immune escape score, TIDE score, and higher PD1&CTLA4 immunophenoscore in ovarian cancer. Moreover, PRS-based risk score acted as an indicator for drug sensitivity in the immunotherapy and chemotherapy of ovarian cancer patients.

Conclusions: All in all, our study developed a prognostic PRS showing powerful and good performance in predicting clinical outcome of ovarian cancer patients. PRS could serve as an indicator for drug sensitivity in the chemotherapy and immunotherapy.

INTRODUCTION

Ovarian cancer is one of the deadliest malignancies among females. An estimated of 22,000 patients are diagnosed with this malignancy in the USA each year, ranking the eleventh most common malignancy and the fifth leading cause of cancer-related death among women [1]. The management of ovarian cancer has shifted from surgery alone to a multi-disciplinary approach including surgery, chemotherapy, endocrine therapy, and immunotherapy. However, the 5-year overall survival (OS) rate for ovarian cancer patients are still less than 50% [2]. High recurrence and drug resistance remain the main reasons leading to the poor clinical outcomes for ovarian cancer patients [3]. Increasing evidences suggest immunotherapy as a promising modality for many malignancies, especially for advanced malignancies [4]. However, few drugs have been approved for the immunotherapy of ovarian cancer, which need to be further investigated. Moreover, limited biomarkers for monitoring the prognosis, drug sensitivity of immunotherapy and chemotherapy have been used for clinical application.

After being activated by other genes, Phosphatidylinositol-4,5-bisphosphate 3-kinase (PI3K) could result in protein kinase B (Akt) binding to the cell membrane in the PI3K/Akt signal transduction pathway [5]. As an intracellular signaling pathway, the PI3K/Akt pathway is correlated to cell cycle, proliferation, cancer and longevity [6]. Moreover, the PI3K/Akt pathway shows significant correlation with glycolysis, hypoxia, apoptosis, epithelial mesenchymal transition (EMT), tumor recurrence, and treatment resistance [5, 7–9]. Attacking the PI3K/Akt signaling pathway is suggested as one of therapeutic strategies in human cancer [10]. Some of genes in the PI3K/Akt signaling pathway have proved to be prognostic biomarkers in ovarian cancer, such KRAS [11]. However, limited studies have fully clarified the role of the PI3K/Akt signaling pathway related genes (PRGs) in the prognosis of ovarian cancer and its correlation with drug sensitivity.

After obtaining PRGs from Kyoto Encyclopedia of Genes and Genomes (KEGG) database, we then explored their expression and prognostic value in ovarian cancer. We then constructed an optimal PI3K/Akt signaling pathway related signature (PRS) for predicting the prognosis of ovarian cancer using 10 machine learning algorithms. Moreover, we also explored the correlation between PRS and tumor microenvironment as well as drug sensitivity in ovarian cancer. Our result may provide more evidences about the significant functions of the PI3K/Akt signaling pathway in the prognosis and drug sensitivity of cancers.

MATERIALS AND METHODS

Datasets sources

Supplementary Figure 1 showed the work flow of our study. Gene sets of PI3K/AKT pathway (n=354) were generated from KEGG PATHWAY Database (https://www.kegg.jp/kegg/pathway.html). RNA sequencing (RNA-seq) data of 374 ovarian cancer patients and 64 normal human ovarian samples were downloaded from TCGA database (https://portal.gdc.cancer.gov/repository) and GTEx database (https://xenabrowser.net/datapages/), respectively. Another five GEO datasets, including GSE14764 (n=80), GSE26193 (n=107), GSE26712 (n=185), GSE63885 (n=75) and GSE140082 (n=380), were used as testing cohorts for prognostic signature validation. The single cell expression data were isolated from GSE184880 dataset, including 5 normal tissues and 7 ovarian cancer tissues. Two immunotherapy cohorts (IMvigor210 (n=298) and GSE91061 (n=98) dataset) containing clinical information about the patients being treated with anti-PD-L1 and anti-CTLA4 agents were used to evaluate the performance of prognostic signature in predicting immunotherapy benefit.

Integrative machine learning algorithms constructed an optimal PRS

After obtaining the differentially expressed genes (DEGs) with "limma" package using $|\text{LogFC}| \geq 1.5$ as the cutoff, we then detected potential prognostic biomarkers for ovarian cancer among PRGs with univariate cox analysis ($p<0.05$). In order to develop an accurate and stable prognostic PRS for ovarian cancer, we then performed integrative analysis with 10 machine learning algorithms, including random survival forest (RSF), elastic network (Enet), Lasso, Ridge, stepwise Cox, CoxBoost, partial least squares regression for Cox (plsRcox), supervised principal components (SuperPC), generalized boosted regression modelling (GBM), and survival support vector machine (survival-SVM). Consistent with a previous study [12] and the link to the R scripts available on the Github website (https://github.com/Zaoqu-Liu/IRLS), we set the TCGA cohort as the training cohort and GEO cohorts as the testing cohort. Harrell's concordance index (C-index) was calculated in all cohorts. The optimal prognostic PRG was regarded as the prognostic model with the highest average C-index. Based on the expression of genes in PRS and their corresponding coefficients, we then calculated the PRS score (risk score) of each OC patient. And OC patients were separated into high risk score and low risk score groups in each cohorts.

Evaluation of the performance of PRS

The cut-off value was determined by the "surv_cutpoint" function of the R package "survminer", which calculated statistics based on maximally selected rank statistics. Using "timeROC" package, we then generated time ROC curves, which could evaluate the performance of PRS in predicting the clinical outcome of ovarian cancer. We also randomly collected 54 prognostic signatures (Supplementary Table 1) that have developed for ovarian cancer and calculated their C-indexes using "rms" package. Moreover, univariate and multivariate cox analysis were performed to identify the risk factors among clinical characters and PRS for the prognosis of ovarian cancer. A predict nomogram based on PRS and clinical characters was constructed for ovarian cancer with "nomogramEx" R package.

Immune infiltration analysis

Immunedeconv, an R package integrating 7 state-of-the-art algorithms, including CIBERSORT, MCPcounter, QUANTISEQ, XCELL, CIBERSORT-ABS, TIMER and EPIC [13], was used to explore the correlation between risk score and abundance of immune cells. The ESTIMATE algorithm was also used to calculate

the Immune score and ESTIMATE score of OC patients by using the R package "estimate" [14].

Drug sensitivity and gene set enrichment analyses

Two approaches, including immunophenoscore and Tumor Immune Dysfunction and Exclusion (TIDE) score, were suggested as reliable tools for predicting immunotherapy response. Immunophenoscore (IPS) of ovarian cancer cases were downloaded from The Cancer Immunome Atlas (TCIA, https://tcia.at/home). And the TIDE score and T cells exclusion scores of ovarian cancer cases were determined by TIDE (http://tide.dfci.harvard.edu). Gene sets of immune escape, immune surveillance and proliferation, were downloaded in previous publication (Supplementary Table 2) [15]. Hallmark gene sets were downloaded from Molecular Signatures Database (MSigDB). Using the R packages "clustersProfiler", "enrichplot", and "ggplot2", we performed Gene Set Enrichment Analyses (GSEA) to improve our understanding of PRS related function and pathways. After downloading the drug sensitivity data of Genomics of Drug Sensitivity in Cancer (GDSC) (https://www.cancerrxgene.org/), we then calculated the half maximal inhibitory concentration (IC50) value of common drugs correlated with chemotherapy and endocrinotherapy of ovarian cancer cases with "oncoPredict" package.

Gaussian mixture and logistic regression models for classifying lymphatic and venous invasion

Lymphatic and venous invasion were vital factors affecting the prognosis of ovarian cancer patients. We then identified the best model among PRS genes to classify lymphatic and venous invasion. Classification was conducted with model-based hierarchical agglomerative clustering based on the Gaussian finite mixture model. The PRS genes related clusters were classified by the Gaussian mixture model (GMM). Logistic regression analysis was performed to construct combined models to classify whether the patients had lymphatic and venous invasion.

Single-cell RNA-seq analysis

ScRNA-seq data were under quality control prior to analysis. Cells with >25% of mitochondria-associated genes were filtered out. The top 2000 highly variable genes of each sample were normalized using the ScaleData function. RunPCA function was used to reduce the dimensionality of the PCA. Using "seurat" package, we then performed T-SNE analysis, which could map high dimensional cellular data into a two-dimensional space, grouping cells with similar expression patterns and separating those with different expression patterns. Cell types were determined by using SingleR method.

Pseudotime analysis and cell-cell interaction analysis

Pseudotime analysis, also named cell trajectory analysis, could evaluate the evolutionary trajectory of apoptosis pathways and cell subtypes and infer the differentiation trajectory of certain cells during disease progression. We performed pseudotime analysis using "Monocle2" package. The pseudotime value was used by monocle to model the gene expression level as a nonlinear smooth pseudotime function to show change in gene expression with time. FDR < 0.05 was regarded as significant difference. We then explored the communication between immune cell subtypes using CellChat software, which contained the ligand-receptor information.

ceRNA network

The upstream miRNA targets of PRS genes were predicted using several databases, including TargetScan, ENCORI, miRDB, RNAIter, TargetMiner, RNA22, miRwalk. And the upstream circRNAs interacting with miRNA were explored with StarBase 3.0.

Statistical analysis

Statistical analyses were conducted with R software (version 4.2.1). Wilcoxon rank-sum test or student T test was performed to explore the difference between continuous variables. Pearson's or Spearman's rank correlation analysis was conducted to analyze the correlations between two continuous variables. The two-sided log-rank test was used to test the difference in different Kaplan-Meier survival curves.

Availability of data and materials

The analyzed data sets generated during the study were sourced from the TCGA database (https://portal.gdc.cancer.gov/repository) and GEO database (https://www.ncbi.nlm.nih.gov/geo).

RESULTS

The relationship of PRGs with ovarian cancer prognosis

As shown in Supplementary Figure 2A, a total of 174 DEGs were obtained in ovarian cancer with |LogFC| ≥ 1.5 as the cutoff (p<0.05). Supplementary Figure 2B showed the top 50 DEGs in ovarian cancer. Among these genes, 29 genes were significantly correlated with the prognosis of ovarian cancer (Figure 1A). To be

more specific, ANGPT2, PPP2R5C, LPAR2, IL2RG, AKT1, CREB3, RHEB, GNG5, and HSP90AA1 were significantly correlated with a good clinical outcome in ovarian cancer (Figure 1A, HR<1, p<0.05). While COL1A1, COL1A2, FN1, CCND1, KRAS, THBS2, COL6A3, ITGB5, LAMB2, AKT2, CSF1R, PDGFRB, CDKN1B, ITGB8, ITGA11, ITGA5, BCL2L11, EFNA5, PDGFRA, and FGF7 were significantly correlated with a poor clinical outcome in ovarian cancer (Figure 1A, HR>1, p<0.05).

Integrative machine learning algorithms developed an optimal prognostic PRS

Above 29 potential prognostic biomarkers were then subjected to an integrative procedure including 10 machine learning-based methods, with which we could develop an accurate and stable prognostic PRS. Aa result, a total of 101 kinds of prediction models were obtained, and their C-index of training cohort (TCGA) and testing cohort (GSE14764, GSE26193, GSE26712, GSE63885 and GSE140082) were shown in Figure 1B. We could see that the model constructed by Lasso + survivalSVM method was considered as the optimal model and they had a highest average C-index of 0.6 (Figure 1B). In the Lasso regression, the optimal λ was obtained when the partial likelihood deviance reached the minimum value based on the LOOCV framework (Figure 1C). A total of 19 genes with nonzero Lasso coefficients were submitted to survivalSVM, which identified a final set of 19 PRS and their coefficients were shown in Figure 1D. Using the cut-off value, we then divided into ovarian cancer cases into high and low risk groups based on their risk scores (PRS score). As expected, ovarian cancer patients with high risk score had a poor OS rate in TCGA (p<0.0001, Figure 1E), GSE14764 (p=0.012, Figure 1F), GSE26193 (p=0.0036, Figure 1G), GSE26712 (p=0.0024, Figure 1H), GSE63885 (p=0.006, Figure 1I) and GSE140082 (p=0.00015, Figure 1J) cohort. tSNE analysis about the classification of ovarian cancer cases into high- and low-risk groups of training cohort and testing cohort were shown in Figure 1K–1P. On the basis of above findings, we concluded that this PRS was capable of predicting the prognosis of ovarian cancer patients.

Evaluation of the performance of PRS

ROC analysis was performed to evaluate the discrimination of PRS in training cohort and testing cohort, with 1-, 3-, and 5-year AUCs of 0.741, 0.718, and 0.738 in TCGA cohort (Figure 2A); 0.620, 0.666, and 0.641 in GSE14764 cohort (Figure 2B); 0.493, 0.568, and 0.552 in GSE26193 cohort (Figure 2C); 0.684, 0.657, and 0.604 in GSE26712 cohort (Figure 2D); 0.569, 0.667, and 0.678 in GSE63885 cohort (Figure 2E), respectively. In GSE140082 cohort, 1-, and 3-year AUCs were 0.550 and 0.640, respectively (Figure 2F). Further univariate and multivariate cox regression analysis demonstrated risk score as an independent risk factor for the prognosis of ovarian cancer patients in TCGA, GSE14764, GSE26193, GSE63885 and GSE140082 cohort (Figure 2G, 2H). We then compared the C-index of our PRS and 54 prognostic signatures that have been established for ovarian cancer. As shown in Supplementary Figure 3A, the C-index of the current PRS was higher than most of 54 random prognostic signatures. All in all, our PRS had a relatively good performance in predicting the clinical outcome of ovarian cancer patients. Considering PRS-based risk score, clinical stage and tumor grade, we then developed a nomogram for predicting the overall survival of ovarian cancer patients (Supplementary Figure 3B), which could help the clinicians evaluate the clinical outcome of ovarian cancer patients and make an appropriate follow-up project. Compared with the idea curve, nomogram-based calibration curves had a relative well predictive value in predicting the 1-, 3-, and 5-year OS rate (Supplementary Figure 3C).

Development of the optimal model for evaluating the status of lymphatic and venous invasion

Lymphatic and venous invasion were vital factors affecting the prognosis of ovarian cancer. We then identified the optimal model among PRS genes to classify lymphatic and venous invasion. Logistic regression analysis was firstly performed to evaluate the association between the expression values of 19 genes in PRS and the AUC values that were screened the status of lymphatic and venous invasion. As a result, a total of 32767 formulas were generated from the logistic regression model. Furthermore, we used decisive GMM-based clustering, a very feasible approach with a good clustering performance [16, 17], to clustered gene sets into eight clusters (lymphatic invasion classifying) or nine clusters (venous invasion classifying) in our proposed algorithm. The cluster that had the highest AUC was considered as the best model to predict the status of lymphatic and venous invasion. As shown in Supplementary Figure 4B, the lymphatic invasion classifying model developed by 10 TRGs (CCND1, CDKN1B, CSF1R, EFNA5, FGF7, HSP90AA1, IL2RG, KRAS, LPAR2, RHEB) had a max AUC of 0.749 by the GMM classifier in one of the 32767 formulas. And venous invasion classifying developed by 11 TRGs (AKT2, CDKN1B, CREB3, CSF1R, EFNA5, FGF7, GNG5, HSP90AA1, ITGA5, ITGB8, RHEB) had a max AUC of 0.816 by the GMM classifier in one of the 32767 formulas (Supplementary Figure 4B).

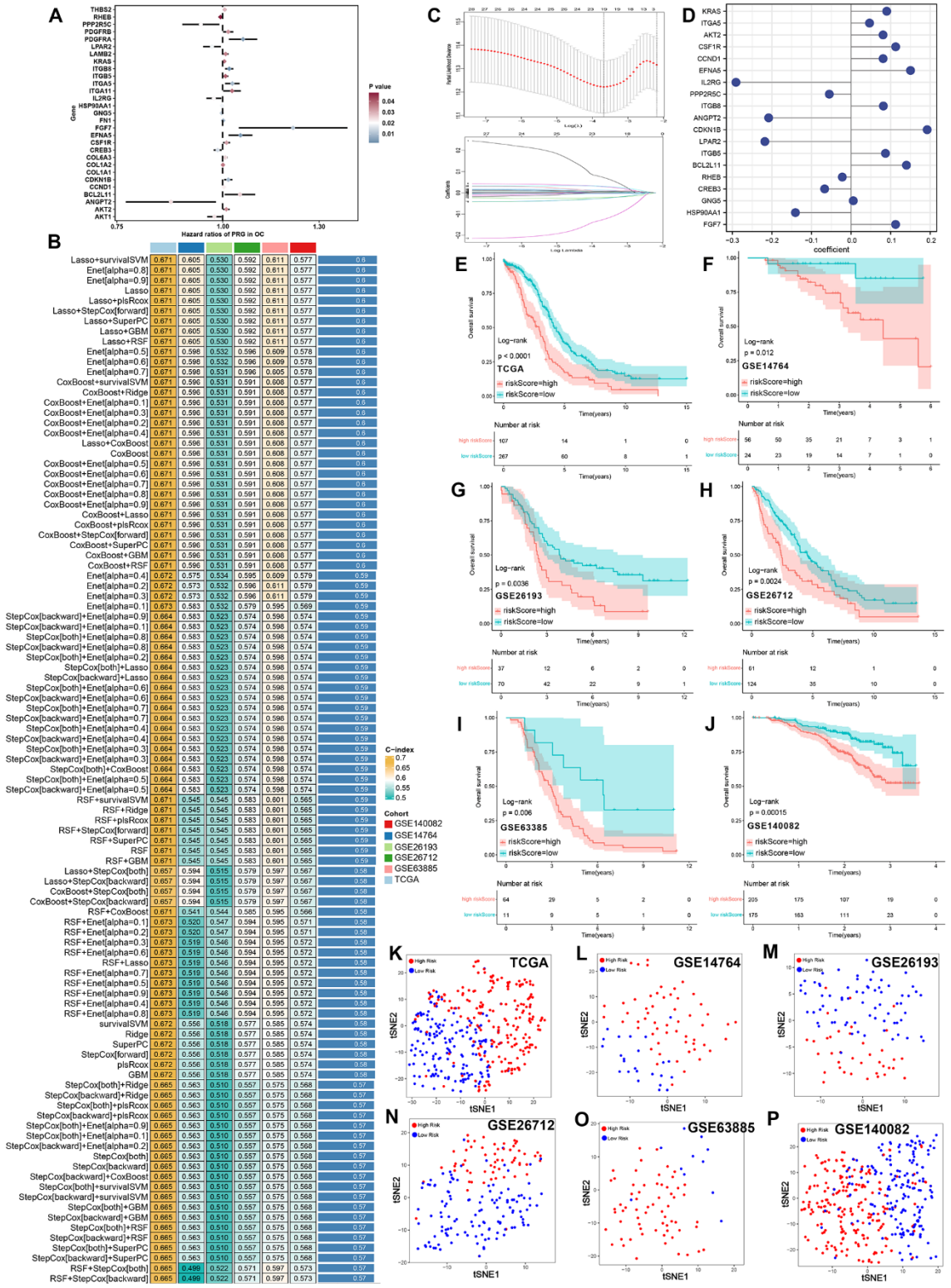

Figure 1. Integrative machine learning analysis constructed a prognostic PI3K/Akt pathway related signature. (**A**) Potential biomarker identified by univariate cox analysis. (**B**) The C-index of 101 kinds prognostic models constructed by 10 machine learning algorithms in training and testing cohort. (**C**) The determination of the optimal λ was obtained when the partial likelihood deviance reached the minimum value, and further generated Lasso coefficients of the most useful prognostic genes. (**D**) Coefficients of 19 genes finally obtained in survivalSVM regression. The survival curve of ovarian cancer with high and low risk score in TCGA (**E**), GSE14764 (**F**), GSE26193 (**G**), GSE26172 (**H**), GSE63885 (**I**) and GSE140082 (**J**) cohort. Cluster analysis of ovarian cancer cases with high and low risk score in TCGA (**K**), GSE14764 (**L**) GSE26193 (**M**), GSE26172 (**N**), GSE63885(**O**) and GSE140082 (**P**) cohort by using tSNE method.

PRS showed significant correlation with cancer-related hallmark

In order to clarify the vital role of PRS in ovarian cancer, we then perform GSEA analysis and explore PRS related biological process and internal connection in ovarian cancer. As expected, ovarian cancer with high risk score had a higher proliferation score, angiogenesis score, DNA repair score, EMT signaling score, Glycolysis score, and Hypoxia score (Figure 3A–3F, all

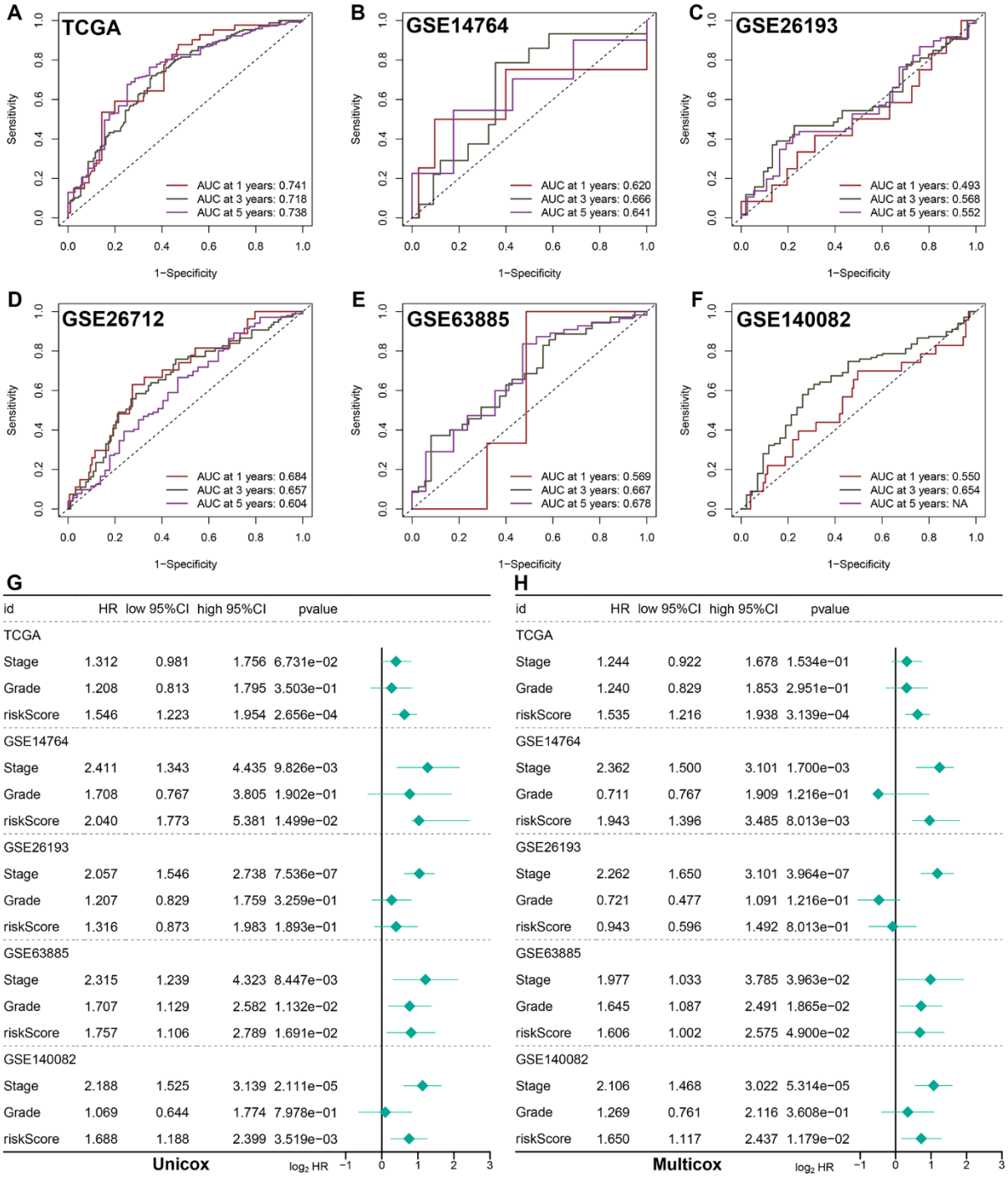

Figure 2. Evaluation of the performance of prognostic PI3K/Akt pathway related signature (PRS). ROC curve evaluated discrimination of PRS in predicting 1-, 3-, and 5-year OS rate of ovarian cancer in TCGA (**A**), GSE14764 (**B**), GSE26193 (**C**), GSE26172 (**D**), GSE63885 (**E**) and GSE140082 (**F**) cohort. (**G**, **H**) Univariate and multivariate cox regression analysis considering grade, stage and risk score in training and testing cohort.

p<0.05). Moreover, high risk score indicated a higher IL2-STAT5 signaling score, IL6-JAK-STAT3 signaling score, NOTCH signaling score, P53 pathway score, and G2M checkpoint score in ovarian cancer (Figure 3G–3K, all p<0.05). Interestingly, apoptosis score was significantly higher in ovarian cancer patients with low risk score (Figure 3L, p=0.028). Increasing evidences have highlighted vital role of macrophages M2/M1 proportion in tumor progression, prognosis and immunotherapy [18–20]. We found that high risk score indicated a higher level of macrophages M2/M1 proportion in TCGA, GSE26193, and GSE26712 cohort (Supplementary Figure 5A–5C, all p<0.05). These results implied that the activation of PI3K/ATK signaling participated in the tumor progression and shortened prognosis in ovarian cancer patients.

The correlation between PRS and tumor microenvironment (TME) in ovarian cancer

Tumor immune landscape could be clustered into six different types, including wound healing (C1), IFN-g dominant (C2), inflammatory (C3), lymphocyte depleted (C4), immunologically quiet (C5) and TGF-b dominant (C6) [21]. As shown in Figure 4A, C2 ranked most of TCGA ovarian cancer cases in both low and high risk group. However, the proportion of C4 in high risk group was significantly higher than that in low risk group (Figure 4A, p=0.001). With several algorithms including CIBERSORT, MCPcounter, QUANTISEQ, XCELL, CIBERSORT-ABS, TIMER and EPIC, we provided insights into the immune landscape in low and high risk groups to avoid inaccuracy and bias caused by

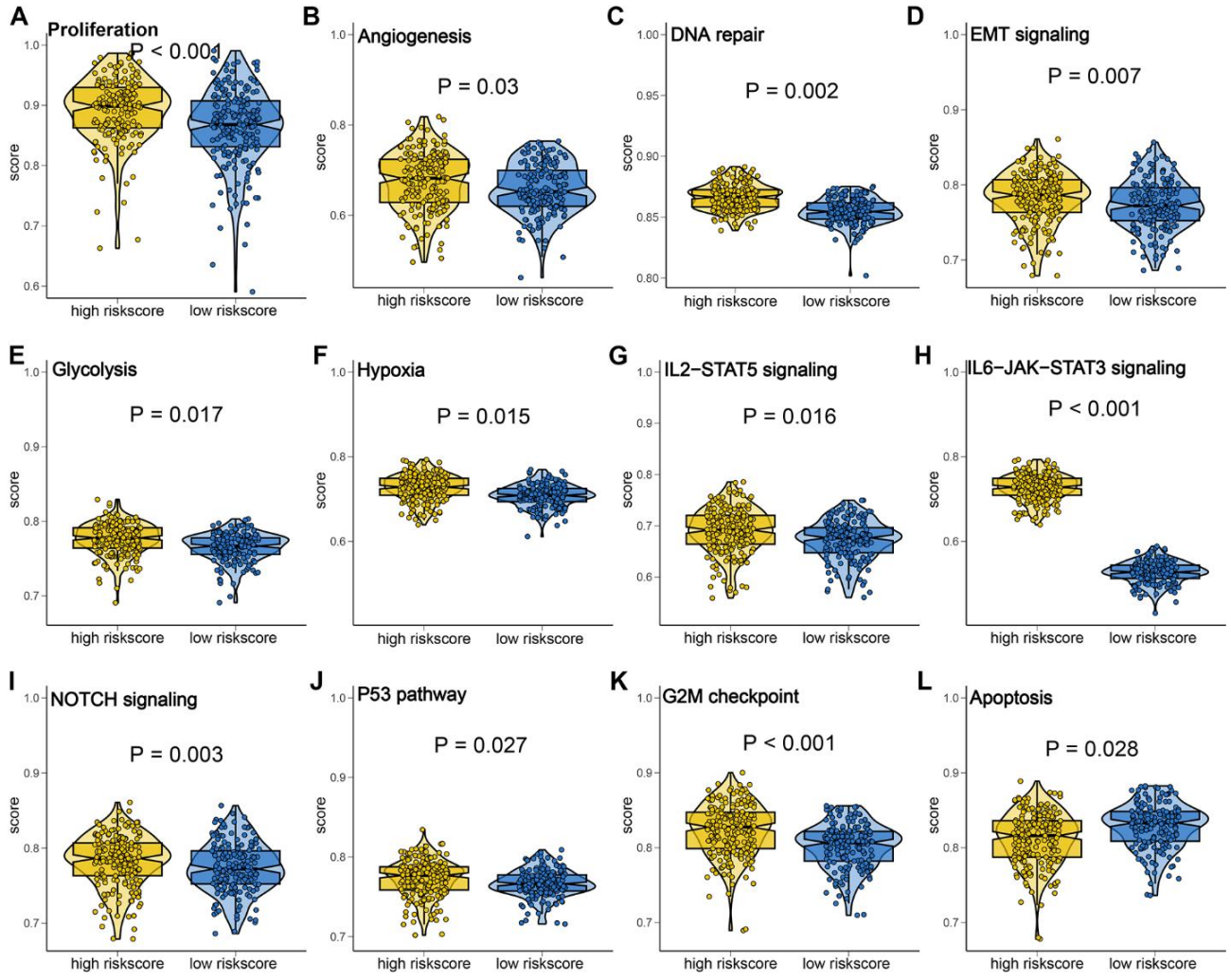

Figure 3. Gene set enrichment analysis of PI3K/Akt pathway related signature (PRS). The gene score of hallmark gene sets correlated with proliferation (**A**), angiogenesis score (**B**), DNA repair score (**C**), EMT signaling score (**D**), Glycolysis score (**E**), Hypoxia score (**F**), IL2-STAT5 signaling score (**G**), IL6-JAK-STAT3 signaling score (**H**), NOTCH signaling score (**I**), P53 pathway score (**J**), G2M checkpoint score (**K**) and apoptosis (**L**) in low and high risk score.

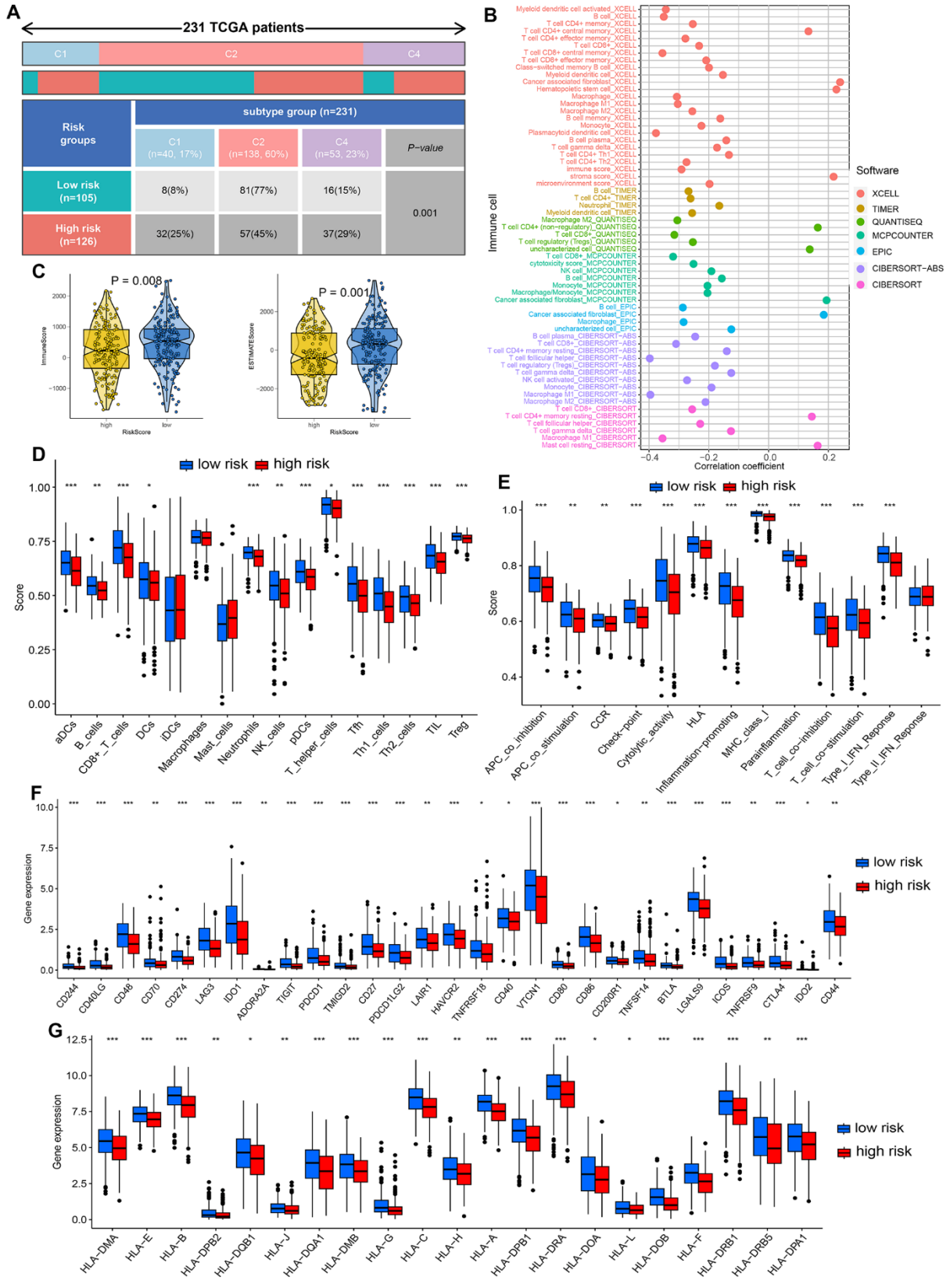

Figure 4. Dissection of PI3K/Akt pathway related signature (PRS)-based tumor microenvironment (TME). (**A**) Tumor immune landscape in ovarian cancer with high and low risk score. (**B**) Correlation between PRS and immune infiltration in ovarian cancer. (**C**) The TME score difference in different risk score group of ovarian cancer. The difference of the score of immune cells (**D**), immune-related functions (**E**), immune checkpoint (**F**), HLA-related genes (**G**) in different risk score group of ovarian cancer. *p<0.05, **p<0.01, ***p<0.001.

the use of a single algorithm. Significant negative correlation was obtained between risk score and the abundance of most immune cells (Figure 4B). As expected, negative correlation was obtained between risk score and the abundance of most immune cells (Figure 4C, all $p<0.05$). As expected, low risk score indicated a higher ESTIMATE score and Immune score in ovarian cancer (Figure 4C, all $p<0.05$). In CIBERSORT algorithm, ovarian cancer with low risk score had a higher level of aDcs, B cells, $CD8^+$ T cells, DCs, neutrophils, NK cells, pDCs, T helper cells, Tfh, Th1 cells, Th2 cells, TIL and Treg (Figure 4D). Moreover, low risk score was associated with a higher score of immune related functions in ovarian cancer, including APC_co_inhibition and stimulation, cytolytic activity, MHC cluss I, parainflammation, T cell co_inhibition, and type_I_IFN_reponse (Figure 4E, all $p<0.05$). Low risk score indicated a higher level of most of HLA-related genes (Figure 4F, $p<0.05$) and immune checkpoints (Figure 4G, $p<0.05$) in ovarian cancer patients. These results suggested that low risk score may be a relatively "hot" tumor phenotype compared with high risk score in ovarian cancer.

Assessment of response to immunotherapy and chemotherapy between high and low risk score group

The above clarified the significant correlation between risk score and TME and the results suggested that ovarian cancer with low risk score may be a relatively "hot" tumor phenotype. Thus, we then explored whether risk score could predict the response to immunotherapy in ovarian cancer. As shown in Figure 5A, 5B, ovarian cancer with high risk score had a higher score of immune escape (Figure 5A, $p<0.001$) and immune surveillance (Figure 5B, $p<0.001$). Higher TIDE score and low IPS scores indicate higher immune escape potential and lower immunotherapy response rates. In our study, high risk score indicated a higher TIDE score (Figure 5C, p=0.005) and T cell exclusion score (Figure 5D, $p<0.001$) in ovarian cancer. IPS was a superior predictor of response to anti-CTLA-4 and anti-PD-1antibodies and high IPS indicated a better response to immunotherapy [22]. The results suggested that ovarian cancer with low risk score had a higher CTLA4 IPS, PD1 IPS and CTLA4/PD1 IPS (Figure 5E, all $p<0.05$). These results suggested that ovarian cancer patients with low risk score may be more sensitive to immunotherapy. In order to verify these results, we then used two immunotherapy cohorts, including IMvigor210 cohort and GSE91061 cohort. As shown in Figure 5F, patients in CR/PR group had a significant lower risk score, with an AUC of 0.83 in ROC curve ($p=0.005$). Interestingly, high risk score was associated with a poor OS rate, with 1-, 2-, and 3-year AUCs of 0.706, 0.712, and 0.718 (Figure 5G). Similar results were obtained in IMvigor210 dataset, which showed that CR/PR group indicated a lower risk score, with an AUC of 0.75 in ROC curve (Figure 5H, $p=0.004$). And patients with high risk score had a poor OS rate, with 1-, and 2- year AUCs of 0.627, 0.846 (Figure 5I, $p<0.001$). These evidences may suggest that ovarian cancer patients with low risk score may be more sensitive to immunotherapy and PRS may be an indicator for immunotherapy response. We then estimated the IC50 value of drugs correlated with chemotherapy and endocrinotherapy between high and low risk score group in order to guide clinical treatment in ovarian cancer. The result suggested that low risk score group tended to benefit from chemotherapy with 5-Fluorouracil, Cisplatin, Cyclophosphamide, Docetaxel, Epirubicin, Gemcitabine, Olaparib, Oxaliplatin, Topotecan, Tamoxifen, Erlotinib and Foretinib (Supplementary Figure 6A–6L, all $p<0.05$).

The correlation between PRS and mutation landscape in ovarian cancer

As genetic mutation played a vital role in tumor genesis and progression. We then compared the difference of mutation landscape in high and low risk score group. Supplementary Figure 7A, 7B showed the mutation landscape of ovarian cancer in these two groups. Patients in low risk score group had a higher tumor mutational burden (TMB) score (Supplementary Figure 7C, $p=0.001$). Moreover, further prognostic analysis revealed that high TMB score and high risk score were associated with a poor OS rate (Supplementary Figure 7D, 7E, $p<0.001$).

High-resolution scRNA-seq revealed the immune landscape of ovarian cancer

A total of 5 normal tissues and 7 ovarian cancer tissues were analyzed to characterize the immune landscape in ovarian cancer. As shown in Figure 6A, all the cells in these tissues could be clustered into 7 subtypes, including T cells, Smooth muscle cells, NK cell, Fibroblasts, Macrophage, NK cell, and Endothelial cells and Monocyte. We then explored the fraction of different immune cell types in each sample, revealing that different immune cell types varied significantly among different samples (Figure 6B). To be specific, T cells were prevalent in tumor tissues while smooth muscle cells were predominant in normal tissues (Figure 6B). Compared with normal tissues, ovarian tissues had a high PRG score (Figure 6C). With the progression of ovarian cancer, the PRG score was increasing (Figure 6D). These results further revealed that the activation of PI3K/ATK signaling participated in the tumor progression and shortened prognosis in ovarian cancer patients. As cancer-associated Fibroblast (CAF) plays a vital role in tumor progression. We then collected Fibroblast in tumor for

further analysis. Using t-SNE analysis, CAF were categorized as myCAF and iCAF cells (Figure 6E). Further analysis revealed a different trajectory between different pseudotime, state, and cell subtypes in the development trajectory analyses of CAF cells (Figure 6F–6H). Figure 6I revealed the expression of PRG in different state of CAF cells.

Cell communication network analysis in ovarian cancer

We studied the signaling pathway that allowed multiple cells to interact with each other during tumorigenesis in order to illustrate how these cells regulate tumorigenesis. The number and strength of interactions

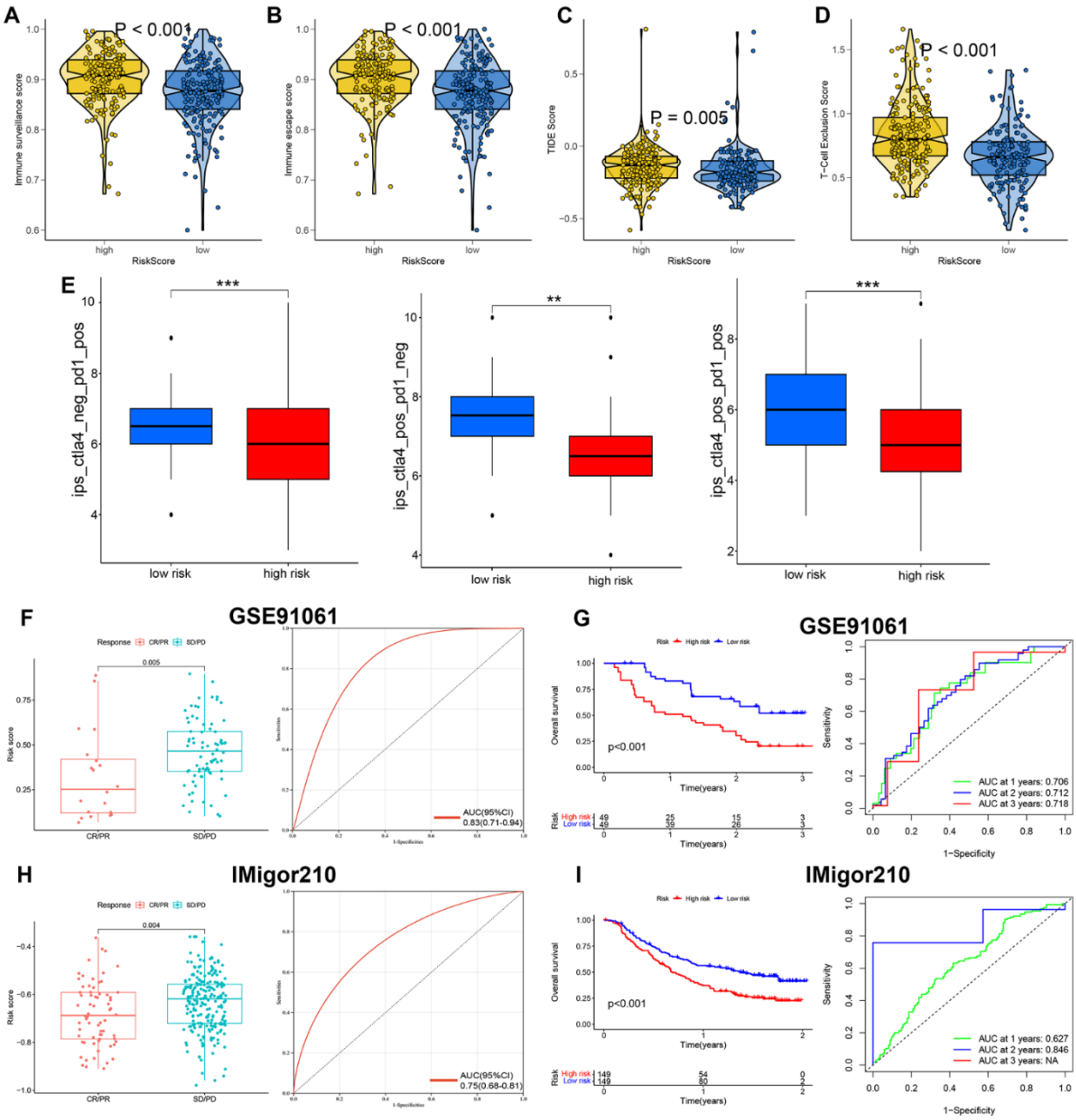

Figure 5. PI3K/Akt pathway related signature (PRS)-based treatment strategy for ovarian cancer. The level of immune surveillance score (**A**), immune escape (**B**), TIDE score (**C**), T cell exclusion score (**D**), and immunophenoscore (**E**) in ovarian cancer patients with high and low risk score. The risk score in CR/PR and SD/PD group and corresponding ROC curve in GSE91061 dataset (**F**). The OS curve and corresponding ROC curve in patients with high and low risk score in GSE91061 dataset (**G**). The risk score in CR/PR and SD/PD group and corresponding ROC curve in IMvigor210 dataset (**H**). The OS curve and corresponding ROC curve in patients with high and low risk score in IMvigor210 dataset (**I**). **p<0.01, ***p<0.001.

were shown in Supplementary Figure 8A. We then focus on interaction number and weights/strength of CAF cells with other cell types. The CAF cells were strongly linked with smooth muscle cell, endothelial cells and Monocyte (Supplementary Figure 8B). Further analysis revealed that PRS genes were involved in FGF signaling network in ovarian cancer. FGF signaling could be activated CAF-CAF interaction (Supplementary Figure 8C, 8D). In FGF signaling, FGF7 and FGFR1 were the ligand and receptor, respectively (Supplementary Figure 8E). FGF7 from CAFs may interact with those smooth muscle cells, endothelial cells and Monocyte have FGFR1 expression (Supplementary Figure 8F).

ceRNA network

The above results revealed that FGF7 may play a vital role in the progression of ovarian cancer. We then explore their upstream targets using several databases. As showed in Supplementary Figure 9A, miR-132-3p, miR-195-5p and miR-18b-5p were suggested as potential miRNA targets of FGF7 based on the result of TargetScan, ENCORI, miRDB, RNAIter, TargetMiner, RNA22, miRwalk. We then explored the upstream circRNAs interacting with miR-132-3p, miR-195-5p and miR-18b-5p. As a result, a total of 91 circRNAs were obtained. The circRNA-miRNA-mRNA network was showed in Supplementary Figure 9B.

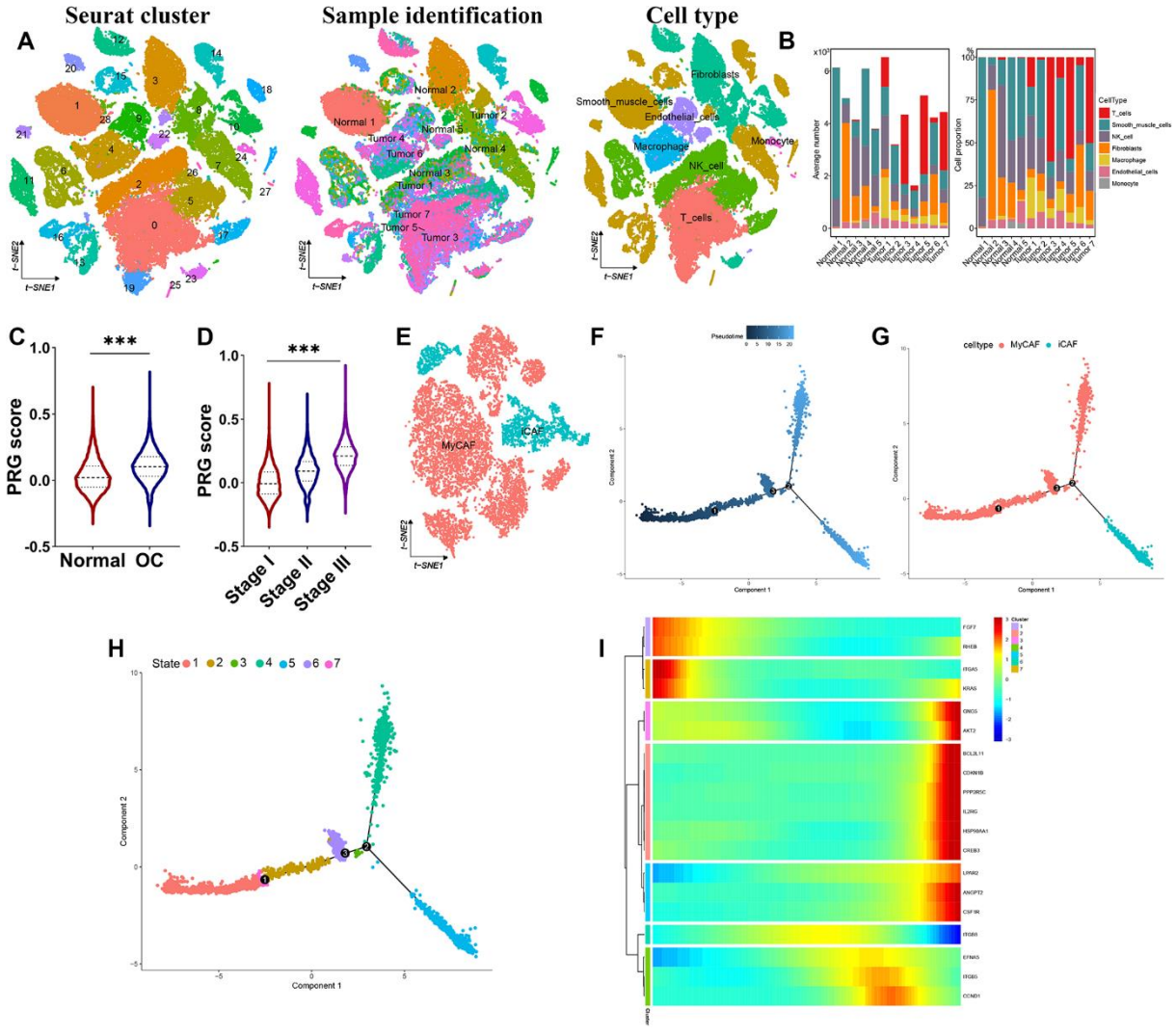

Figure 6. High-resolution revealing immune landscape of ovarian cancer. (**A**) t-SNE plot showing the identified cell types of all ovarian cancer and normal sample. (**B**) Fraction of cell types originating from each sample. (**C**, **D**) PI3K/Akt pathway related signature score in normal sample and ovarian cancer tissues. (**E**) Further sub-cell types of CAF cells. (**F**–**H**) Developmental trajectory of CAF cells inferred by monocle, colored by pseudotime, cell subtype and state. (**I**) Heatmap of the expression of PI3K/Akt pathway related signature genes in the developmental trajectory of CAF cells state. ***p<0.001.

DISCUSSION

Ovarian cancer is one of the most common malignancies among women and its prognosis is poor [23]. Increasing evidences suggest the vital role of the PI3K/Akt pathway in cell cycle, proliferation, cancer, longevity, prognosis and therapy of cancer [24–27]. Moreover, the PI3K/Akt pathway showed significant correlation with glycolysis, hypoxia, apoptosis, epithelial mesenchymal transition (EMT), tumor recurrence, and treatment resistance [5, 7–9]. However, few studies have comprehensively and systematically described the characteristics of the PI3K/Akt pathway related genes in ovarian cancer.

Differentially expressed analysis identified 174 differentially expressed genes (DEGs) of the PI3K/Akt pathway in ovarian cancer. Among these DEGs, a total of 29 genes were significantly correlated with the prognosis of ovarian cancer. We then performed an integrative pipeline including 10 machine learning algorithms, which could develop a powerful prognostic PRS. As a result, the model constructed by Lasso + survivalSVM method was considered as the optimal model with the highest average C-index of 0.6. Moreover, further analysis suggested TRS as an independent risk factor for the overall survival of ovarian cancer patients. Actually, many prognostic models had been constructed for ovarian cancer, including Immune-related LncRNA signature [28], glycometabolism-related signature [29], oxidative stress-related signature [30], transcription factors-based signature [31], ferroptosis-related signature [32] and invasion-related gene signature [33]. In order to compare the performance of these prognostic signatures in evaluating the prognosis of ovarian cancer, we then calculated their C-index. Interestingly, the C-index of PRS was higher than most of other signatures, suggesting that our PRS may have a better performance in predicting the prognosis of ovarian cancer patients.

Immune cell recruitment to the tumor microenvironment is a promising therapeutic strategy, even in aggressive tumors. Increasing evidences have highlighted the vital role of the PI3K/ATK pathway in clinical management of cancer [34, 35]. Conventional chemotherapeutics exert tumor-suppressive effects mainly by inducing the release of DMAPs from cancer cells, activating the presentation of DC cells, thus activating $CD8^+$ T cells to kill cancer cells. The efficacy of these immunotherapy agents and their correlation with the PI3K/ATK pathway [36, 37]. In order to further clarify the role of PRS in TME, we applied several algorithms to explore the underlying association of PRS with immune infiltration. As a result, some immune cells, including T cells, B cells, myeloid dendritic cells, and neutrophils, were more active in PRS-based low risk score group. Moreover, some cancer-related hallmarks were more active in PRS-based high risk score group, including proliferation, angiogenesis, DNA repair, EMT signaling, Glycolysis, Hypoxia, NOTCH signaling, and P53 pathway. These evidences identified that PRS might be involved in the development of ovarian cancer by regulating tumor immunity.

Targeting immune checkpoint molecules can activate anti-tumor immunity to help clear tumors [38].

Immunotherapy has revolutionized the situation of patients with unresectable cancers [39]. Until now, limited effective biomarkers for predicting immunotherapy efficacy have been used clinically, though some biomarkers, including PD-1, PD-L1, MSI, TMB etc., have been identified. Since significant correlation was obtained between PRS and immune infiltration, we further explored the role of PRS in predicting immunotherapy efficacy. As an increased TIDE score indicates a greater likelihood of immune escape and less effectiveness of ICI treatment [40]. IPS was a superior predictor of response to anti-CTLA-4 and anti-PD-1 antibodies and high IPS indicated a better response to immunotherapy [22]. In our study, ovarian cancer with high risk score had a higher immune escape score, higher immune surveillance score, higher TIDE, lower TMB and lower IPS scores. It seems reasonable to assume that patients with PRS-based low risk score benefit more from immunotherapy in terms of the treatment strategies for ovarian cancer. Further studies suggested that the risk score in CR/PR group was lower than that in SD/PD group in GSE91061 and IMvigor210 dataset, which further verifies our results.

Chemotherapy and endocrine therapy were vital therapeutic measures of ovarian cancer. Chemoresistance was one of the most reasons leading to treatment failure of ovarian cancer [41]. The result suggested that low risk group tended to benefit from chemotherapy and endocrine therapy with 5-Fluorouracil, Cisplatin, Cyclophosphamide, Docetaxel, Epirubicin, Gemcitabine, Olaparib, Oxaliplatin, Topotecan, Tamoxifen, Erlotinib and Foretinib, demonstrating that PRS was an indicator for the chemotherapy response of ovarian cancer.

Some limitations and shortcomings remain in our study. All data are obtained from public databases and it would be better to validate this prognostic model using clinical data. Moreover, the mechanism of PRS related genes in the progression of ovarian cancer remains unknown. A more in-depth investigation of these genes in ovarian cancer development will be undertaken *in vivo* or *in vitro*.

CONCLUSIONS

All in all, our study developed a prognostic PRS showing powerful and good performance in predicting the clinical outcome of ovarian cancer patients. PRS could serve as an indicator for drug sensitivity in chemotherapy and immunotherapy.

AUTHOR CONTRIBUTIONS

Xiaofang Han performed data analysis work and aided in writing the manuscript. Xiaofang Han and Liu Yang designed the study, assisted in writing the manuscript. Hui Tian and Yuanyuan Ji edited the manuscript. All authors read and approved the final manuscript.

CONFLICTS OF INTEREST

The authors declare that they have no conflicts of interest.

FUNDING

This study was funded by the Natural Science Foundation of Shanxi Province (201901D111443).

REFERENCES

1. Morand S, Devanaboyina M, Staats H, Stanbery L, Nemunaitis J. Ovarian Cancer Immunotherapy and Personalized Medicine. Int J Mol Sci. 2021; 22:6532. https://doi.org/10.3390/ijms22126532 PMID:34207103

2. Armstrong DK, Alvarez RD, Backes FJ, Bakkum-Gamez JN, Barroilhet L, Behbakht K, Berchuck A, Chen LM, Chitiyo VC, Cristea M, DeRosa M, Eisenhauer EL, Gershenson DM, et al. NCCN Guidelines® Insights: Ovarian Cancer, Version 3.2022. J Natl Compr Canc Netw. 2022; 20:972–80. https://doi.org/10.6004/jnccn.2022.0047 PMID:36075393

3. Liang L, Yu J, Li J, Li N, Liu J, Xiu L, Zeng J, Wang T, Wu L. Integration of scRNA-Seq and Bulk RNA-Seq to Analyse the Heterogeneity of Ovarian Cancer Immune Cells and Establish a Molecular Risk Model. Front Oncol. 2021; 11:711020. https://doi.org/10.3389/fonc.2021.711020 PMID:34621670

4. Zhang Y, Zhang Z. The history and advances in cancer immunotherapy: understanding the characteristics of tumor-infiltrating immune cells and their therapeutic implications. Cell Mol Immunol. 2020; 17:807–21. https://doi.org/10.1038/s41423-020-0488-6 PMID:32612154

5. Xie Y, Shi X, Sheng K, Han G, Li W, Zhao Q, Jiang B, Feng J, Li J, Gu Y. PI3K/Akt signaling transduction pathway, erythropoiesis and glycolysis in hypoxia (Review). Mol Med Rep. 2019; 19:783–91. https://doi.org/10.3892/mmr.2018.9713 PMID:30535469

6. Ma L, Zhang R, Li D, Qiao T, Guo X. Fluoride regulates chondrocyte proliferation and autophagy via PI3K/AKT/mTOR signaling pathway. Chem Biol Interact. 2021; 349:109659. https://doi.org/10.1016/j.cbi.2021.109659 PMID:34536393

7. Xu W, Yang Z, Lu N. A new role for the PI3K/Akt signaling pathway in the epithelial-mesenchymal transition. Cell Adh Migr. 2015; 9:317–24. https://doi.org/10.1080/19336918.2015.1016686 PMID:26241004

8. Jin Y, Chen Y, Tang H, Hu X, Hubert SM, Li Q, Su D, Xu H, Fan Y, Yu X, Chen Q, Liu J, Hong W, et al. Activation of PI3K/AKT Pathway Is a Potential Mechanism of Treatment Resistance in Small Cell Lung Cancer. Clin Cancer Res. 2022; 28:526–39. https://doi.org/10.1158/1078-0432.CCR-21-1943 PMID:34921019

9. Noorolyai S, Shajari N, Baghbani E, Sadreddini S, Baradaran B. The relation between PI3K/AKT signalling pathway and cancer. Gene. 2019; 698:120–8. https://doi.org/10.1016/j.gene.2019.02.076 PMID:30849534

10. Yu L, Wei J, Liu P. Attacking the PI3K/Akt/mTOR signaling pathway for targeted therapeutic treatment in human cancer. Semin Cancer Biol. 2022; 85:69–94. https://doi.org/10.1016/j.semcancer.2021.06.019 PMID:34175443

11. Nodin B, Zendehrokh N, Sundström M, Jirström K. Clinicopathological correlates and prognostic significance of KRAS mutation status in a pooled prospective cohort of epithelial ovarian cancer. Diagn Pathol. 2013; 8:106. https://doi.org/10.1186/1746-1596-8-106 PMID:23800114

12. Liu Z, Liu L, Weng S, Guo C, Dang Q, Xu H, Wang L, Lu T, Zhang Y, Sun Z, Han X. Machine learning-based integration develops an immune-derived lncRNA signature for improving outcomes in colorectal cancer. Nat Commun. 2022; 13:816. https://doi.org/10.1038/s41467-022-28421-6 PMID:35145098

13. Li T, Fu J, Zeng Z, Cohen D, Li J, Chen Q, Li B, Liu XS. TIMER2.0 for analysis of tumor-infiltrating immune cells. Nucleic Acids Res. 2020; 48:W509–14.

https://doi.org/10.1093/nar/gkaa407
PMID:32442275

14. Yoshihara K, Shahmoradgoli M, Martínez E, Vegesna R, Kim H, Torres-Garcia W, Treviño V, Shen H, Laird PW, Levine DA, Carter SL, Getz G, Stemke-Hale K, et al. Inferring tumour purity and stromal and immune cell admixture from expression data. Nat Commun. 2013; 4:2612.
https://doi.org/10.1038/ncomms3612 PMID:24113773

15. Sun Y, Wu L, Zhong Y, Zhou K, Hou Y, Wang Z, Zhang Z, Xie J, Wang C, Chen D, Huang Y, Wei X, Shi Y, et al. Single-cell landscape of the ecosystem in early-relapse hepatocellular carcinoma. Cell. 2021; 184:404–21.e16.
https://doi.org/10.1016/j.cell.2020.11.041
PMID:33357445

16. Ficklin SP, Dunwoodie LJ, Poehlman WL, Watson C, Roche KE, Feltus FA. Discovering Condition-Specific Gene Co-Expression Patterns Using Gaussian Mixture Models: A Cancer Case Study. Sci Rep. 2017; 7:8617.
https://doi.org/10.1038/s41598-017-09094-4
PMID:28819158

17. Hong HC, Chuang CH, Huang WC, Weng SL, Chen CH, Chang KH, Liao KW, Huang HD. A panel of eight microRNAs is a good predictive parameter for triple-negative breast cancer relapse. Theranostics. 2020; 10:8771–89.
https://doi.org/10.7150/thno.46142
PMID:32754277

18. Dan H, Liu S, Liu J, Liu D, Yin F, Wei Z, Wang J, Zhou Y, Jiang L, Ji N, Zeng X, Li J, Chen Q. RACK1 promotes cancer progression by increasing the M2/M1 macrophage ratio via the NF-κB pathway in oral squamous cell carcinoma. Mol Oncol. 2020; 14:795–807.
https://doi.org/10.1002/1878-0261.12644
PMID:31997535

19. Sun M, Zeng H, Jin K, Liu Z, Hu B, Liu C, Yan S, Yu Y, You R, Zhang H, Chang Y, Liu L, Zhu Y, et al. Infiltration and Polarization of Tumor-associated Macrophages Predict Prognosis and Therapeutic Benefit in Muscle-Invasive Bladder Cancer. Cancer Immunol Immunother. 2022; 71:1497–506.
https://doi.org/10.1007/s00262-021-03098-w
PMID:34716763

20. Wang H, Yung MMH, Ngan HYS, Chan KKL, Chan DW. The Impact of the Tumor Microenvironment on Macrophage Polarization in Cancer Metastatic Progression. Int J Mol Sci. 2021; 22:6560.
https://doi.org/10.3390/ijms22126560
PMID:34207286

21. Thorsson V, Gibbs DL, Brown SD, Wolf D, Bortone DS, Ou Yang TH, Porta-Pardo E, Gao GF, Plaisier CL, Eddy JA, Ziv E, Culhane AC, Paull EO, et al, and Cancer Genome Atlas Research Network. The Immune Landscape of Cancer. Immunity. 2018; 48:812–30.e14.
https://doi.org/10.1016/j.immuni.2018.03.023
PMID:29628290

22. Charoentong P, Finotello F, Angelova M, Mayer C, Efremova M, Rieder D, Hackl H, Trajanoski Z. Pan-cancer Immunogenomic Analyses Reveal Genotype-Immunophenotype Relationships and Predictors of Response to Checkpoint Blockade. Cell Rep. 2017; 18:248–62.
https://doi.org/10.1016/j.celrep.2016.12.019
PMID:28052254

23. Wang JY, Lu AQ, Chen LJ. LncRNAs in ovarian cancer. Clin Chim Acta. 2019; 490:17–27.
https://doi.org/10.1016/j.cca.2018.12.013
PMID:30553863

24. Akbarzadeh M, Mihanfar A, Akbarzadeh S, Yousefi B, Majidinia M. Crosstalk between miRNA and PI3K/AKT/mTOR signaling pathway in cancer. Life Sci. 2021; 285:119984.
https://doi.org/10.1016/j.lfs.2021.119984
PMID:34592229

25. He Y, Sun MM, Zhang GG, Yang J, Chen KS, Xu WW, Li B. Targeting PI3K/Akt signal transduction for cancer therapy. Signal Transduct Target Ther. 2021; 6:425.
https://doi.org/10.1038/s41392-021-00828-5
PMID:34916492

26. Mortazavi M, Moosavi F, Martini M, Giovannetti E, Firuzi O. Prospects of targeting PI3K/AKT/mTOR pathway in pancreatic cancer. Crit Rev Oncol Hematol. 2022; 176:103749.
https://doi.org/10.1016/j.critrevonc.2022.103749
PMID:35728737

27. Stefani C, Miricescu D, Stanescu-Spinu II, Nica RI, Greabu M, Totan AR, Jinga M. Growth Factors, PI3K/AKT/mTOR and MAPK Signaling Pathways in Colorectal Cancer Pathogenesis: Where Are We Now? Int J Mol Sci. 2021; 22:10260.
https://doi.org/10.3390/ijms221910260
PMID:34638601

28. Pan X, Bi F. A Potential Immune-Related Long Non-coding RNA Prognostic Signature for Ovarian Cancer. Front Genet. 2021; 12:694009.
https://doi.org/10.3389/fgene.2021.694009
PMID:34367253

29. Liu L, Cai L, Liu C, Yu S, Li B, Pan L, Zhao J, Zhao Y, Li W, Yan X. Construction and Validation of a Novel Glycometabolism-Related Gene Signature Predicting Survival in Patients With Ovarian Cancer. Front Genet. 2020; 11:585259.
https://doi.org/10.3389/fgene.2020.585259
PMID:33281878

30. Zhang J, Yang L, Xiang X, Li Z, Qu K, Li K. A panel of three oxidative stress-related genes predicts overall survival in ovarian cancer patients received platinum-based chemotherapy. Aging (Albany NY). 2018; 10:1366–79. https://doi.org/10.18632/aging.101473 PMID:29910195

31. Cheng Q, Li L, Yu M. Construction and validation of a transcription factors-based prognostic signature for ovarian cancer. J Ovarian Res. 2022; 15:29. https://doi.org/10.1186/s13048-021-00938-2 PMID:35227285

32. Wang H, Cheng Q, Chang K, Bao L, Yi X. Integrated Analysis of Ferroptosis-Related Biomarker Signatures to Improve the Diagnosis and Prognosis Prediction of Ovarian Cancer. Front Cell Dev Biol. 2022; 9:807862. https://doi.org/10.3389/fcell.2021.807862 PMID:35071242

33. Liang L, Li J, Yu J, Liu J, Xiu L, Zeng J, Wang T, Li N, Wu L. Establishment and validation of a novel invasion-related gene signature for predicting the prognosis of ovarian cancer. Cancer Cell Int. 2022; 22:118. https://doi.org/10.1186/s12935-022-02502-4 PMID:35292033

34. Duan Y, Haybaeck J, Yang Z. Therapeutic Potential of PI3K/AKT/mTOR Pathway in Gastrointestinal Stromal Tumors: Rationale and Progress. Cancers (Basel). 2020; 12:2972. https://doi.org/10.3390/cancers12102972 PMID:33066449

35. Vasan N, Cantley LC. At a crossroads: how to translate the roles of PI3K in oncogenic and metabolic signalling into improvements in cancer therapy. Nat Rev Clin Oncol. 2022; 19:471–85. https://doi.org/10.1038/s41571-022-00633-1 PMID:35484287

36. Guerrero-Zotano A, Mayer IA, Arteaga CL. PI3K/AKT/mTOR: role in breast cancer progression, drug resistance, and treatment. Cancer Metastasis Rev. 2016; 35:515–24. https://doi.org/10.1007/s10555-016-9637-x PMID:27896521

37. Mayer IA, Arteaga CL. The PI3K/AKT Pathway as a Target for Cancer Treatment. Annu Rev Med. 2016; 67:11–28. https://doi.org/10.1146/annurev-med-062913-051343 PMID:26473415

38. Dai Y, Qiang W, Lin K, Gui Y, Lan X, Wang D. An immune-related gene signature for predicting survival and immunotherapy efficacy in hepatocellular carcinoma. Cancer Immunol Immunother. 2021; 70:967–79. https://doi.org/10.1007/s00262-020-02743-0 PMID:33089373

39. Riley RS, June CH, Langer R, Mitchell MJ. Delivery technologies for cancer immunotherapy. Nat Rev Drug Discov. 2019; 18:175–96. https://doi.org/10.1038/s41573-018-0006-z PMID:30622344

40. Fu J, Li K, Zhang W, Wan C, Zhang J, Jiang P, Liu XS. Large-scale public data reuse to model immunotherapy response and resistance. Genome Med. 2020; 12:21. https://doi.org/10.1186/s13073-020-0721-z PMID:32102694

41. Tian W, Lei N, Zhou J, Chen M, Guo R, Qin B, Li Y, Chang L. Extracellular vesicles in ovarian cancer chemoresistance, metastasis, and immune evasion. Cell Death Dis. 2022; 13:64. https://doi.org/10.1038/s41419-022-04510-8 PMID:35042862

SUPPLEMENTARY MATERIALS

Supplementary Figures

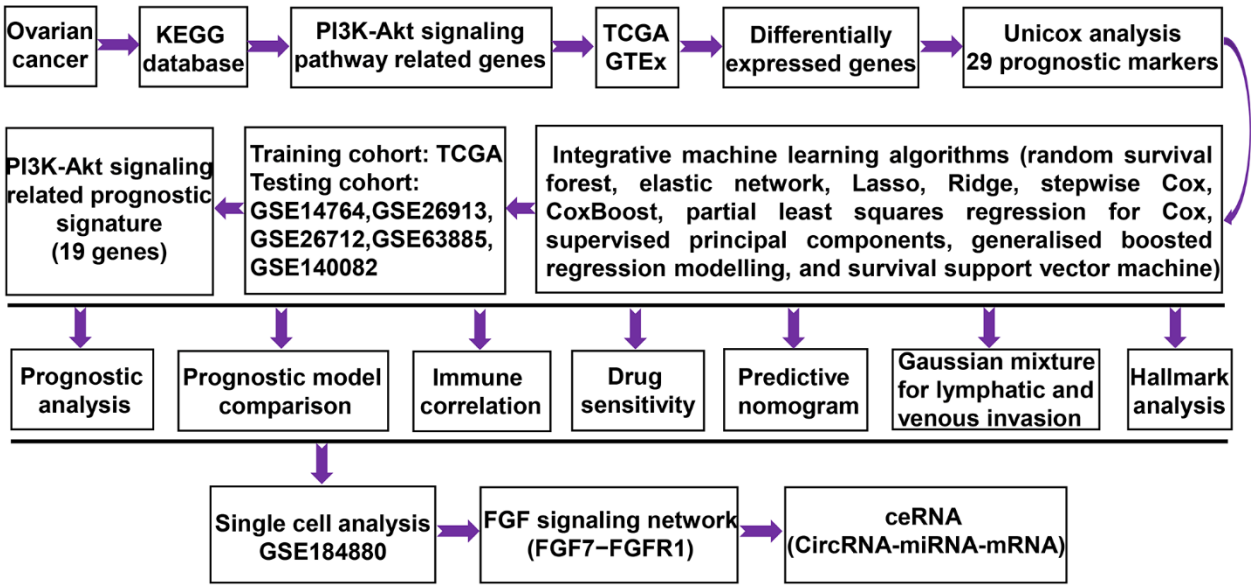

Supplementary Figure 1. Study workflow.

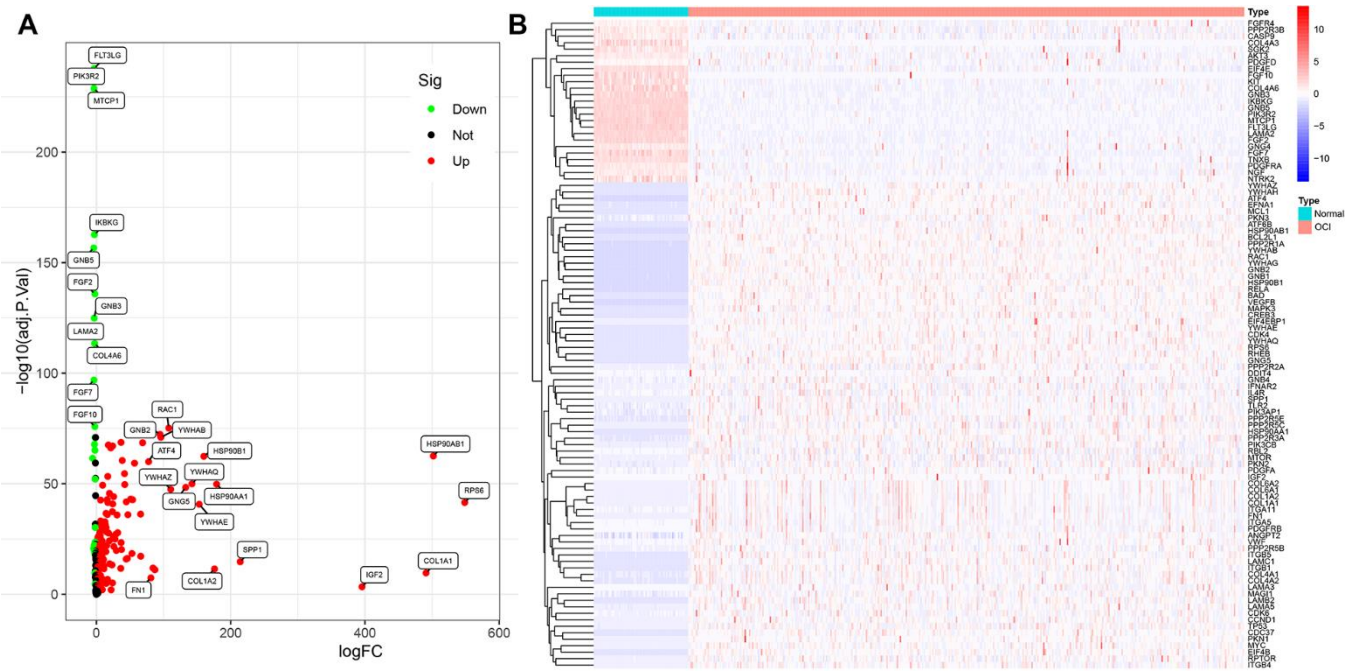

Supplementary Figure 2. Differentially expressed genes between ovarian cancer and normal tissues. (**A**) Volcanic map showed all differentially expressed genes in ovarian cancer among PI3K/Akt pathway related genes. (**B**) Heatmap showed top 50 differentially expressed genes in ovarian cancer among PI3K/Akt pathway related genes.

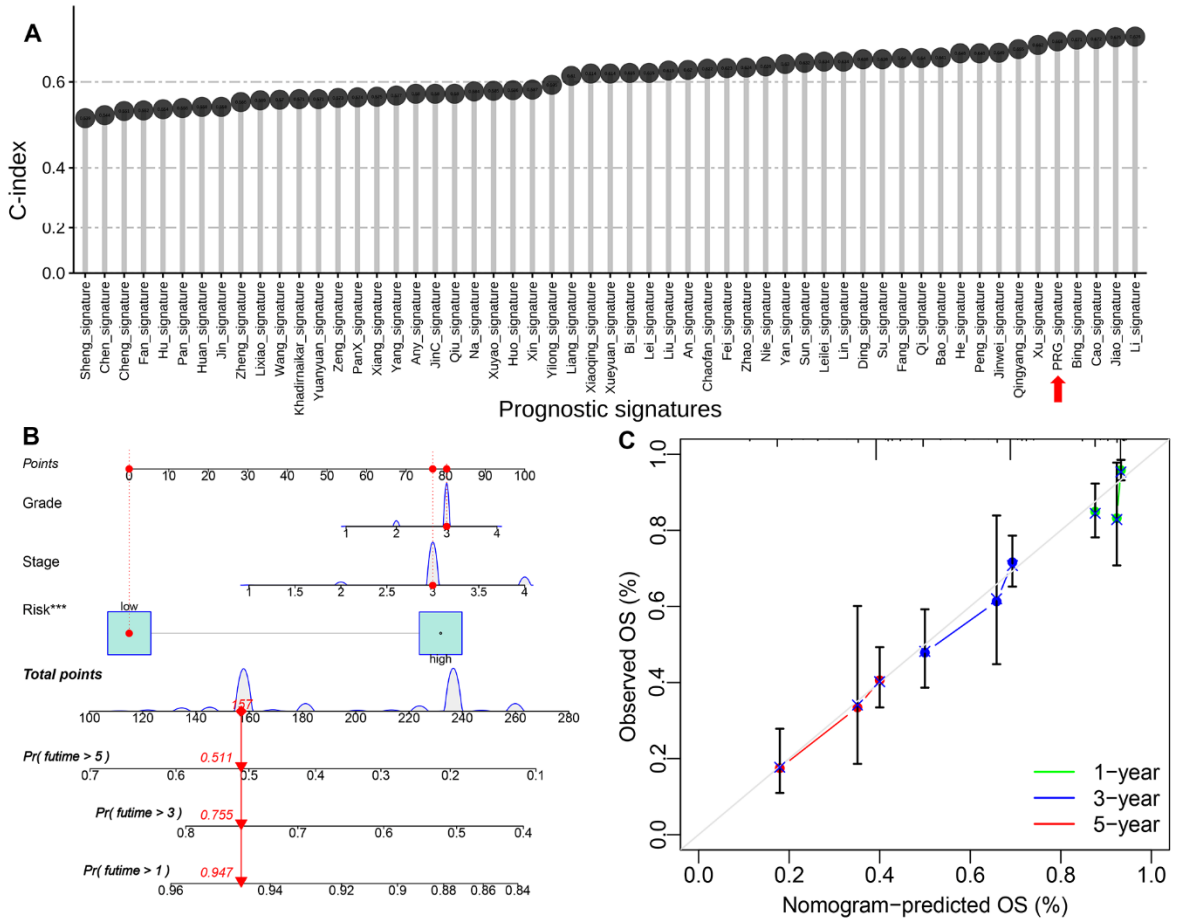

Supplementary Figure 3. The performance of prognostic PI3K/Akt pathway related signature (PRS) in predicting the prognosis of ovarian cancer. (**A**) C-index of PRS and other established signatures evaluated the prognosis of ovarian cancer patients. (**B**, **C**) Prediction nomogram for predicting the 1-, 3-, and 5-year OS rate of ovarian cancer.

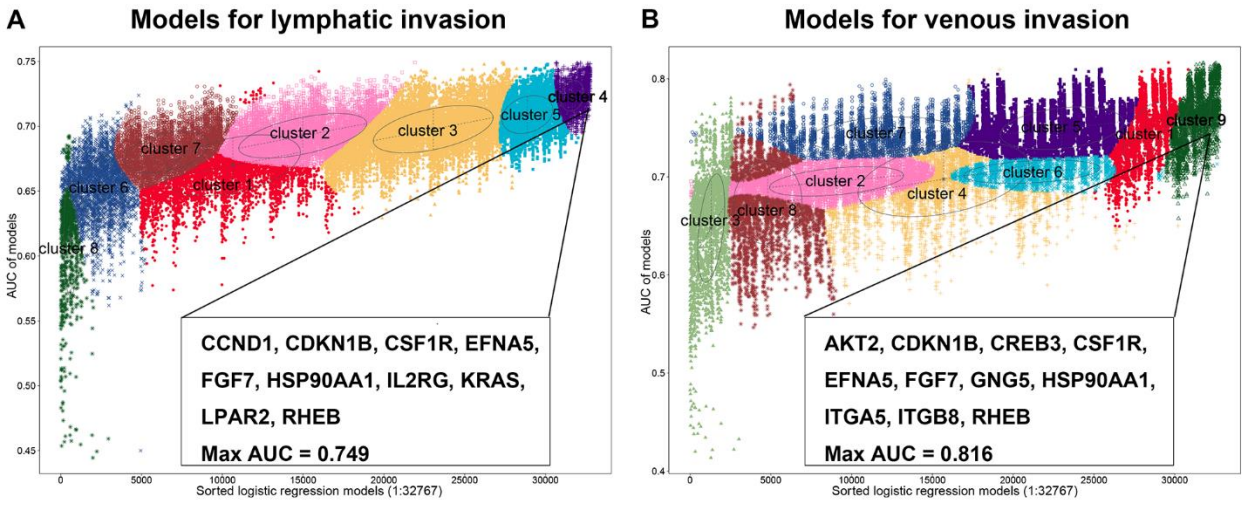

Supplementary Figure 4. The pattern of AUC and logistic regression models was based on Gaussian finite mixture models for classifying lymphatic and venous invasion. The pattern of the logistic regression model correlated with the AUC scores and was identified by a Gaussian mixture for classifying lymphatic (**A**) and venous invasion (**B**).

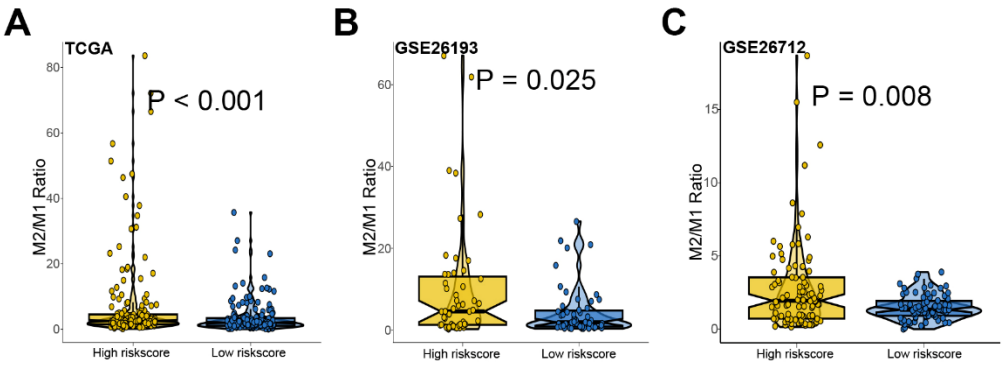

Supplementary Figure 5. The level of macrophages M2/M1 proportion in ovarian cancer patients with high and low risk score in TCGA (**A**), GSE26193 (**B**) and GSE26712 (**C**) cohort.

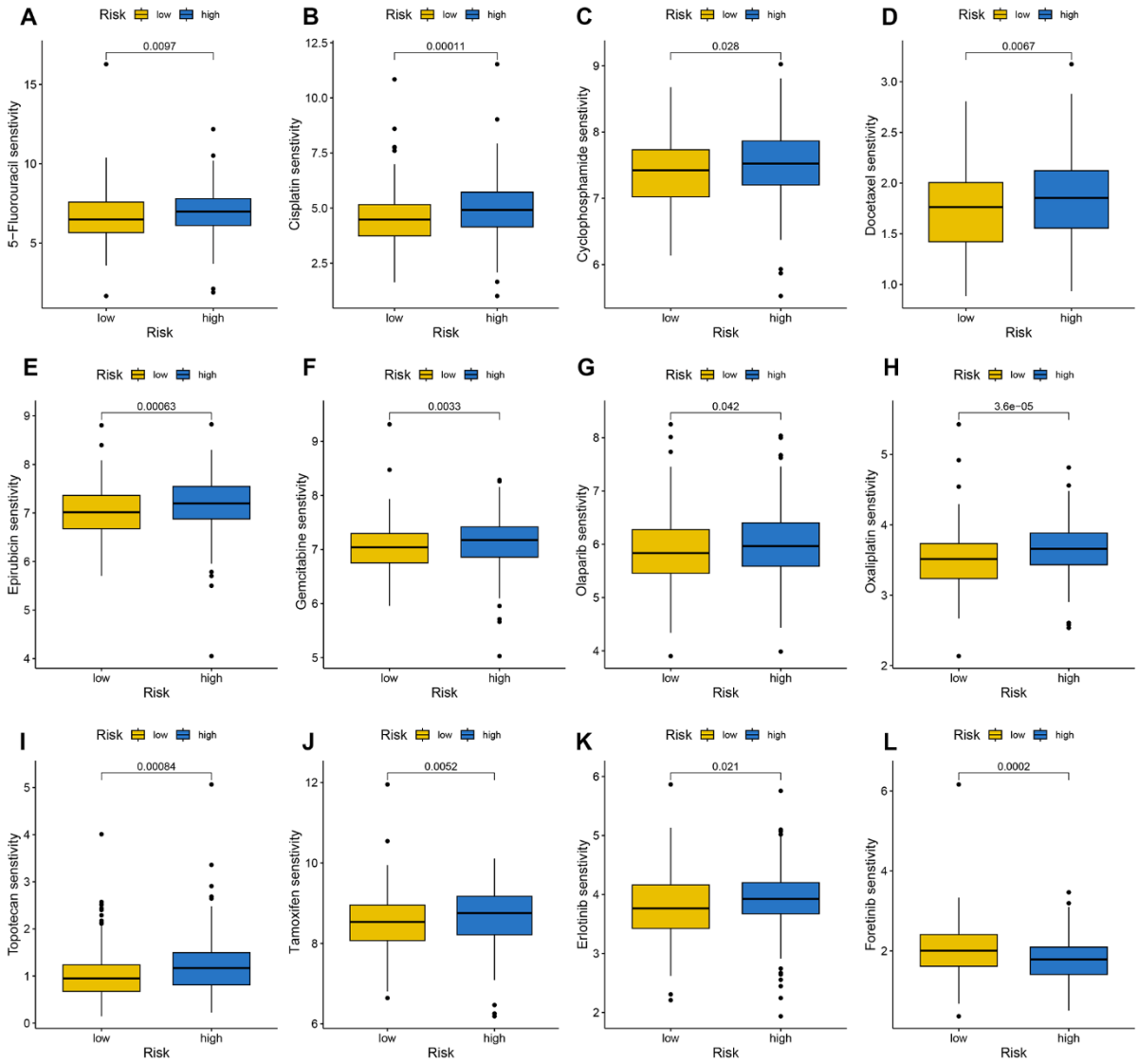

Supplementary Figure 6. PI3K/Akt pathway related signature (PRS)-based treatment strategy for ovarian cancer. The IC50 values of 5-Fluorouracil (**A**), Cisplatin (**B**), Cyclophosphamide (**C**), Docetaxel (**D**), Epirubicin (**E**), Gemcitabine (**F**), Olaparib (**G**), Oxaliplatin (**H**), Topotecan (**I**), Tamoxifen (**J**), Erlotinib (**K**), and Foretinib (**L**) in different risk score group of ovarian cancer.

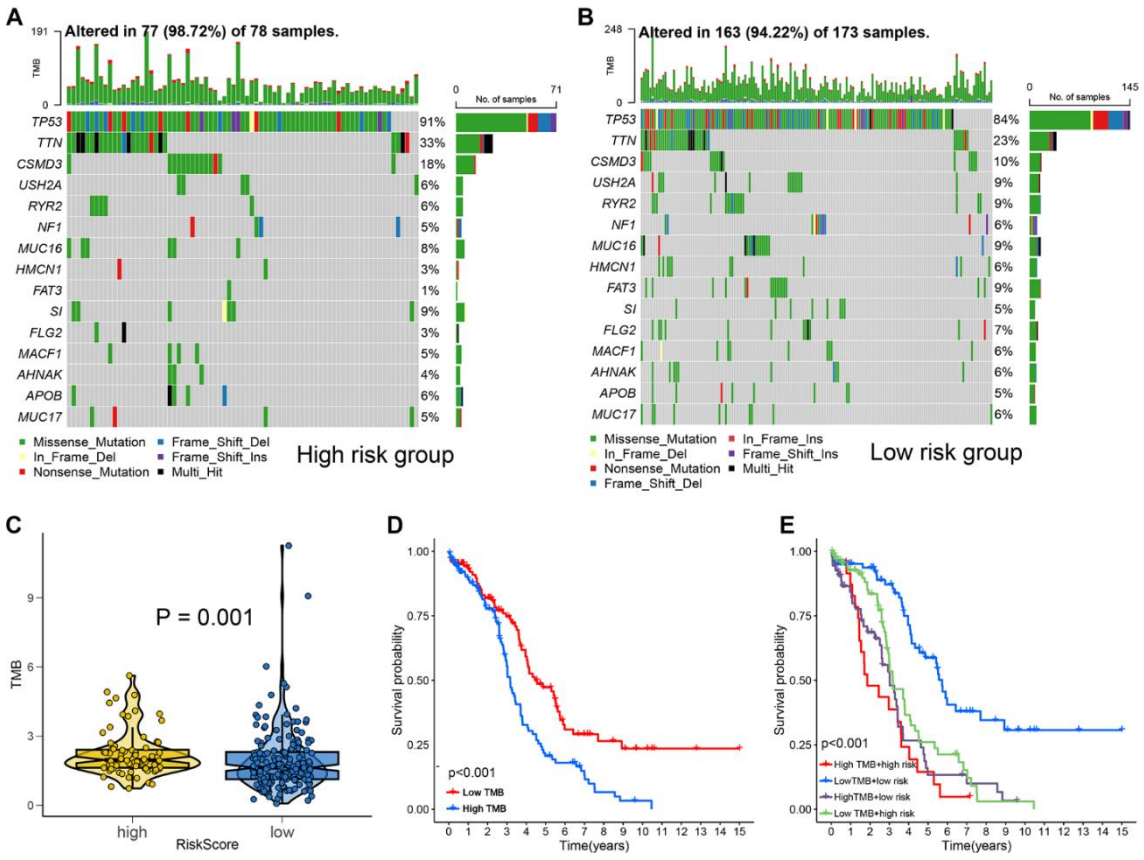

Supplementary Figure 7. Dissection of PI3K/Akt pathway-related signature (PRS)-based genetic mutation. (**A**, **B**) Genetic landscape in different risk score group of ovarian cancer. (**C**) The tumor mutational burden score in different risk score of ovarian cancer. (**D**, **E**) The overall survival curve in ovarian cancer patients with different tumor mutational burden and risk score.

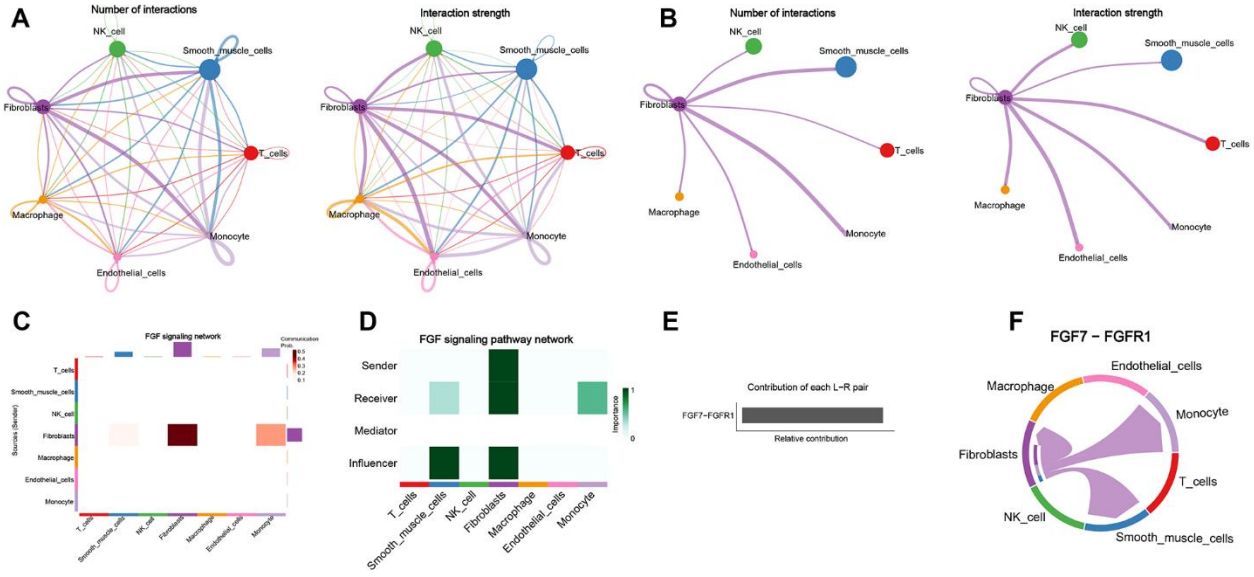

Supplementary Figure 8. Cell communication network analysis in ovarian cancer. (**A**) Chord plot showing the number and weights/strength of interactions among all cell types. (**B**) The interaction number and weights/strength of CAF cells with other cell types. (**C**, **D**) The interaction of all cell types in PI3K/Akt pathway related signature (PRS) related FGF signaling network. (**E**) The sender and receiver pair in FGF signaling network. (**F**) Chart showing inferred intercellular communication network of FGF signaling pathway in all cell types.

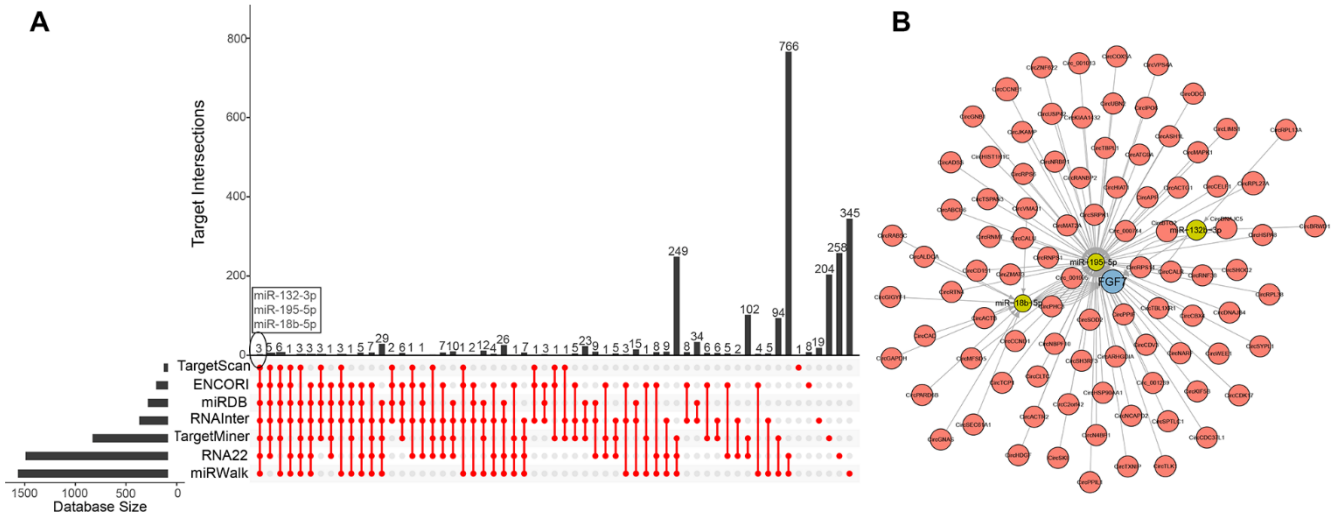

Supplementary Figure 9. ceRNA network associated with hub gene FGF7. (**A**) miRNA target of FGF7 predicted by TargetScan, ENCORI, miRDB, RNAIter, TargetMiner, RNA22, miRwalk. (**B**) circRNA interacting with miRNA predicted by StarBase 3.0 and the circRNA-miRNA-miRNA.

Supplementary Tables

Please browse Full Text version to see the data of Supplementary Table 2.

Supplementary Table 1. Other models had been established for ovarian cancer.

Signature	Title	PMID
An	Development of a Novel Autophagy-related Prognostic Signature for Serous Ovarian Cancer	30410611
Any	The Comprehensive Analysis of Interferon-Related Prognostic Signature with regard to Immune Features in Ovarian Cancer.	35769811
Bao	Novel gene signatures for prognosis prediction in ovarian cancer	32666642
Bi	Establishment of a novel glycolysis-related prognostic gene signature for ovarian cancer and its relationships with immune infiltration of the tumor microenvironment	34496868
Bing	Novel Model for Comprehensive Assessment of Robust Prognostic Gene Signature in Ovarian Cancer Across Different Independent Datasets	31681404
Cao	Development of a multi-gene-based immune prognostic signature in ovarian cancer	33509250
Chaofan	Establishment and validation of an RNA binding protein-associated prognostic model for ovarian cancer	33550985
Chen	Integrating cell cycle score for precise risk stratification in ovarian cancer	36061171
Cheng	Construction and validation of a transcription factors-based prognostic signature for ovarian cancer.	35227285
Ding	Construction of a new tumor immunity-related signature to assess and classify the prognostic risk of ovarian cancer	33154188
Fan	A newly defined risk signature, consisting of three m6A RNA methylation regulators, predicts the prognosis of ovarian cancer	32950970
Fang	Establishment, immunological analysis, and drug prediction of a prognostic signature of ovarian cancer related to histone acetylation	36172179
Fei	Construction autophagy-related prognostic risk signature to facilitate survival prediction, individual treatment and biomarker excavation of epithelial ovarian cancer patients.	33676525
He	Development of a novel transcription factors-related prognostic signature for serous ovarian cancer	33785763
Hu	Identification of a five-gene signature of the RGS gene family with prognostic value in ovarian cancer.	33845140
Huan	Integrated Analysis of Ferroptosis-Related Biomarker Signatures to Improve the Diagnosis and Prognosis Prediction of Ovarian Cancer	35071242
Huo	Identification of a Prognostic Signature for Ovarian Cancer Based on the Microenvironment Genes	34054929
Jiao	N6-Methyladenosine-Related RNA Signature Predicting the Prognosis of Ovarian Cancer.	34137363
Jin	A panel of three oxidative stress-related genes predicts overall survival in ovarian cancer patients received platinum-based chemotherapy	29910195
JinC	A 2-Protein Signature Predicting Clinical Outcome in High-Grade Serous Ovarian Cancer	28976449
Jinwei	Identification and verification of a ten-gene signature predicting overall survival for ovarian cancer	32805252
Khadirnaikar	Development and validation of an immune prognostic signature for ovarian carcinoma	32794637
Lei	Identification of an energy metabolism-related gene signature in ovarian cancer prognosis	32186777
Leilei	Establishment and validation of a novel invasion-related gene signature for predicting the prognosis of ovarian cancer.	35292033
Li	Identification and validation of a gene-based signature reveals SLC25A10 as a novel prognostic indicator for patients with ovarian cancer	36114504
Liang	A Novel Glycosyltransferase-Related Gene Signature for Overall Survival Prediction in Patients with Ovarian Cancer	34992448
Lin	A methylation-driven genes prognostic signature and the immune microenvironment in epithelial ovarian cancer.	35783253
Liu	Construction and validation of a novel aging-related gene signature and prognostic nomogram for predicting the overall survival in ovarian cancer.	34825509
Lixiao	Construction and Validation of a Novel Glycometabolism-Related Gene Signature Predicting Survival in Patients With Ovarian Cancer.	33281878
Na	Comprehensive Analysis of Tumor Microenvironment Identified Prognostic Immune-Related Gene Signature in Ovarian Cancer	33679883
Nie	Prognostic signature of ovarian cancer based on 14 tumor microenvironment-related genes	34260536

Pan	A Potential Immune-Related Long Non-coding RNA Prognostic Signature for Ovarian Cancer	34367253
PanX	A Novel Six-Gene Signature for Prognosis Prediction in Ovarian Cancer	33193589
Peng	A prognostic model based on immune-related long noncoding RNAs for patients with epithelial ovarian cancer	35031063
Qi	A nine-gene signature related to tumor microenvironment predicts overall survival with ovarian cancer	32208363
Qingyang	Identifying the Role of Oxidative Stress-Related Genes as Prognostic Biomarkers and Predicting the Response of Immunotherapy and Chemotherapy in Ovarian Cancer.	36561981
Qiu	A Liquid-Liquid Phase Separation-Related Gene Signature as Prognostic Biomarker for Epithelial Ovarian Cancer	34168991
Sheng	Integrative network analysis identifies an immune-based prognostic signature as the determinant for the mesenchymal subtype in epithelial ovarian cancer.	33031300
Su	A novel immune-related prognostic signature in epithelial ovarian carcinoma	33819196
Sun	Identification of a Prognostic Signature Associated With DNA Repair Genes in Ovarian Cancer.	31572446
Wang	Development of a five-gene signature as a novel prognostic marker in ovarian cancer.	30569721
Xiang	Construction of a prognostic signature for serous ovarian cancer based on lactate metabolism-related genes.	36185201
Xiaoqing	Identification of immunity- and ferroptosis-related genes for predicting the prognosis of serous ovarian cancer	35777713
Xin	The cuproptosis-related gene signature serves as a potential prognostic predictor for ovarian cancer using bioinformatics analysis	36267774
Xu	Integration of Transcriptome and Epigenome to Identify and Develop Prognostic Markers for Ovarian Cancer	36081667
Xueyuan	Derivation, Comprehensive Analysis, and Assay Validation of a Pyroptosis-Related lncRNA Prognostic Signature in Patients With Ovarian Cancer	35280739
Xuyao	A signature based on glycosyltransferase genes provides a promising tool for the prediction of prognosis and immunotherapy responsiveness in ovarian cancer	36611197
Yan	Development and Verification of an Autophagy-Related lncRNA Signature to Predict Clinical Outcomes and Therapeutic Responses in Ovarian Cancer	34671615
Yilong	Identification of a novel ferroptosis-related gene signature associated with prognosis, the immune landscape, and biomarkers for immunotherapy in ovarian cancer	36386203
Yang	Integrated analysis of a competing endogenous RNA network reveals an 11-lncRNA prognostic signature in ovarian cancer	33223503
Yuanyuan	Development and Validation of an Immune-Related Prognostic Signature for Ovarian Cancer Based on Weighted Gene Coexpression Network Analysis	33381581
Zeng	Identification of a Gene Signature of Cancer-Associated Fibroblasts to Predict Prognosis in Ovarian Cancer	35873482
Zhao	Exploration of the Immunotyping Landscape and Immune Infiltration-Related Prognostic Markers in Ovarian Cancer Patients.	35880167
Zheng	Identification three LncRNA prognostic signature of ovarian cancer based on genome-wide copy number variation	32000042

Supplementary Table 2. Signature related gene sets.